IEEE Access
Multidisciplinary ⋮ Rapid Review ⋮ Open Access Journal

Received 24 May 2023, accepted 1 July 2023, date of publication 5 July 2023, date of current version 12 July 2023.

Digital Object Identifier 10.1109/ACCESS.2023.3292795

RESEARCH ARTICLE

Visibility Framework and Performance Analysis for Free Space Optical Communications in Satellite Links

JAVIER GARCÍA OLMEDO AND VÍCTOR P. GIL JIMÉNEZ, (Senior Member, IEEE)
Department of Signal Theory and Communications, Universidad Carlos III de Madrid, Leganés, 28911 Madrid, Spain

Corresponding author: Javier García Olmedo (jgolmedo96@gmail.com)

This work was supported in part by the Project "IRENE" [Ministerio de Asuntos Económicos y Transformación Digital (MINECO)/Agencia Estatal de Investigación (AEI)/Fondo Europeo de Desarrollo Regional (FEDER), Unión Europea (UE)] under Grant PID2020-115323RB-C33); and in part by the Project Madrid Flight on Chip (MFOC)—Innovation Cooperative Projects Comunidad of Madrid—HUBS 2018/Madrid Flight on Chip.

ABSTRACT This paper studies and provides a performance analysis for the atmospheric influence on the visibility in Free Space Optical Communications (FSOC). With a focus on ground station-satellite links, it aims to present and analyse the most commonly used attenuation models for the main atmospheric events, establish relationships and dependence never analyzed before, such as for example in the case of rain and snow. As the characterisation of atmospheric attenuation is far from following a pattern in different locations, this work is intended to simplify and unify all the atmospheric events, proposing the visibility as the main single parameter to compare and analyze them. This parameter is available in most of the measurements, including in the fog scenarios. Besides, the effects of clouds are also analyzed, establishing relationships to visibility, in the case of attenuation calculations, suggesting the use of certain attenuation models and providing a new technique for the calculation of the link blockage in the presence of clouds, which are reported by aviation codes in meteorological stations. Besides, all the sites accessed to obtain the meteorological parameters and tools used for the study in this paper are listed in section II.

INDEX TERMS Attenuation, free space optical communications, link blockage, visibility.

I. INTRODUCTION

It is well known that the interest in Free Space Optical Communications (FSOC) is attracting much of attention recently but it was started 30 years ago when scientists were looking for an alternative or a powerful complement to Radio Frequency Communications (RFC). The most attractive advantage of FSOC is that it can reach data rates of the order of Gbps easily due to the large bandwidth available. For this reason, in addition to a high bandwidth, lower power and mass requirements [1], it can be a technology that provides interesting solutions in many areas. For example, FSOC can be a solution for the high data rates that require the 5G services as well as ensuring the connectivity of a large number of devices in IoT applications [2]. Combining it with RF and 5G, it can result in Vehicle to Vehicle (V2V) or Vehicle-to-Infrastructure (V2I) Communications. For instance, in [3] a study of an uplink Visible Light Communication (VLC) beacon system for the Universal Traffic Management System (UTMS) beneath the National Police Agency of Japan is presented, where V2V and V2I Communications are supported. Another V2V example is presented in [4], specifically, an approach to establish a high-speed broadcast communication link between autonomous underwater vehicles (AUVs) under sea ice.

Having high throughput networks is useful in case of natural disasters or events that require high data rates due to the amount of users, and it can be accomplished combining FSOC with WLAN and Global System for Mobile Communication (GSM) [5] or other cellular system. Besides, it can be used combined with WLAN and Digital Video Broadcasting - Terrestrial (DVB-T) to provide an alternative access

The associate editor coordinating the review of this manuscript and approving it for publication was Parul Garg.

technique to Internet in areas with low coverage [6]. On the other side, FSOC is a powerful option for the Next Generation Passive Optical Networks (NG-PONs), for example, different research have been carried out in literature about the usage of quantum dash lasers in FSOC for applications such as radio over FSOC, indoor data centers or building-to-building communication [7].

It is highly likely that FSOC will play an important role in the following years as the amount of scientific data returning back to Earth is very large and backup systems could be necessary in numerous scenarios, such as the tracking and data satellites relay or a free space optical communication network. This commitment to free-space optical communications technologies can be seen in the National Aeronautics and Space Administration's (NASA) roadmap. For example, the high data rate transmission of the Lunar Laser Demonstration Relay (LLCD) during the years 2013-2014, by using the Laser Communications Relay Demonstration (LCRD) launched in 2021 and certified obtained successful results. That experiment tested and refined the laser systems by NASA, the TeraByte InfraRed Delivery (TBIRD) launched as payload of the Pathfinder Technology Demonstrator 3 (PTD-3) on May of 2022, demonstrating the benefits of space laser communications, to the Integrated LCRD Low-Earth Orbit User Modem. Next year the Amplifier Terminal (ILLUMA-T) as well as the Orion Artemis II Optical Communications System (O2O) are scheduled. Joint together they will transmit for the first time ever high-resolution images and video when the astronauts return to the lunar region after more than 50 years [8].

However, an important disadvantage of FSOC appears in Earth-to-satellite or between multiple optical ground stations (OGS) communications. It is desirable to take into account the effects of the atmospheric channel because it can lead to signal degradation and consequently a link outage. For these reasons, it is an important topic of study in ongoing missions.

The estimation of the specific attenuation of atmospheric events for the design of FSOC links is a challenging task because the needed parameters are not easy to obtain. For example, the most appropriate method for the estimation of the aerosol scattering attenuation, which is the most significant in FSOC, due to fog, is to use Mie's scattering theory [9]. However, parameters such as the refractive index or the particle sizes are not very common to find. It may also not be available for any location, not to mention the computational complexity.

In the case of other atmospheric events, such as the rain or the snow, numerous research have been carried out for many years, resulting in different models that mainly relate the specific attenuation to the precipitation intensity rate and the particles shapes and sizes. Nevertheless, as the measurements of the observations has a wide range of variations depending on the location, the most suitable option is not clear. As an illustration, in the case of rain there are four recommended models by the International Telecommunication Union – Radio Communication Sector (ITU-R), each one with different attenuation trends, even for scenarios where the rainfall meets certain rainfall intensity ranges.

There are many papers that discuss the impact of the atmospheric conditions in FSOC. In [10] the impact of atmospheric conditions in Istanbul is analyzed based not only on aerosol scattering attenuation, but also on molecular absorption and geometrical attenuation, among others. However, they deal with the effects of rain and snow based on the precipitation intensity rate with one model for each event, in contrast with our work that analyzes various models of rain and snow, reformulating them to be based on the visibility. References [11] and [12] discuss the impact of the atmospheric conditions from a wavelength dependence and visibility point of view, providing some performance analysis of the link budget and optimal distance for optical links in several conditions. However, the only atmospheric event covered there, is the fog, with just one or two models, clearly more dedicated to test the effects on the performance of an optical link under this atmospheric event. In [13] an optical system performance is also analyzed under fog conditions. Regarding the use of atmospheric data, [14] uses the National Oceanic and Atmospheric Administration (NOAA) data to analyze the effects of visibility under fog in South Africa and [10] uses atmospheric data from the Istanbul airport. However, the data are used in analyses of areas of particular interest to the authors, and do not consider other locations where conditions vary according to their geographical position. In [15] the research is more focused in the micro-physic and the empiric models of the attenuation and the visibility, in which, the wavelength dependence is also taken into account as well as the fog conditions, further extending the number of fog models and effects depending also on visibility models, not considering the rain and the snow. From the best knowledge of the authors, there are no other paper in the literature that make a distinction between daytime and night time visibility and at the same time characterize the aerosol scattering attenuation due to all the atmospheric events in the channel for multiple locations, also considering the non-availability of an optical link.

In order to solve the aforementioned issues, the goal of this paper is to analyze the different methods and models for estimating the specific attenuation of aerosol scattering due to the most usual and damaging events for FSOC such as fog, snow, rain, and clouds. Besides, due to the variety of models and methods for each of the atmospheric events and to ease the calculations, the use of a single parameter is of great help. In this case, the use of the visibility as a common parameter in a general model for various events is proposed. This parameter is widely available in many airport and meteorological databases, and it is already used in fog attenuation models. In this way, regardless of location, the estimation can be obtained in a simple way to characterize potential areas for FSOC.

The main advantage of using a single parameter for these calculations is that site experiments and measurements are not needed, because the automatic data reports from meteorological and airport stations can be accessed more easily and are available for the entire globe, unlike other parameters that depend on more specific measurements and are only available for very particular locations. On the other hand, it is to be said that there may be variations in estimating the relationship between the visibility and the precipitation rate, but the aim of this work is the ease of access and generalization of attenuation at a large number of locations.

The work presented in this paper compares the main atmospheric attenuation models under the same conditions and analyses their behaviour. Moreover, the unification of a selection of these models under the visibility parameter is proposed, which it results in an easier way to characterize these events in a preliminary study. It is important to note that this paper presents a brief review of atmospheric attenuation models, as well as other parameters involved in the process. However, we would like to point out that this paper is not intended to be a survey, but rather an useful tool (like handbook) in which the main characteristics of the models are described for a better understanding and use.

The main contributions of this paper can be summarized as follows.

- A review on the most important models for atmospheric events applied to an optical satellite link is presented and summarized. To the best knowledge of the authors, there is no other article where all of them are included and related.
- The derivation of all the models (snow, rain, clouds, fog) based on a single parameter such as the visibility is developed. So far, only fog models was based on this parameter. We have generalized into a single formula. We have integrated the models of these events under a single formula, in a way that allows them to be better simplified under the premise of characterising multiple locations in a general way.
- A method for calculating the attenuation of the previously mentioned atmospheric phenomena with the reports of civil and airport meteorological stations is obtained.
- A method for calculating the unavailability of an optical ground station for many locations around the globe with the reports of civil and airport meteorological stations has also been proposed.

The remainder of this document is organized as follows. Section II presents the data sources of meteorological parameters that have been used for this paper. Section III introduces a theoretical background about the visibility and the atmospheric attenuation. Section IV presents and analyses the main atmospheric events and its models from the point of view of the FSOC. For completeness Section V presents the results of the calculations for fog, clouds and all three atmospheric events: fog, rain and snow based only on the proposed parameter, the visibility. Finally, in Section VI our conclusions are presented.

TABLE 1. Collection of meteorological websites.

Websites	Comments
Iowa Environmental Mesonet (IEM) by Iowa State University [16]	This website maintains and provides access to data of databases of ASOS, AWOS, and METAR
State Meteorological Agency (AEMET) - Spanish Government [17]	Meteorological data in various formats (e.g., historical, statistical...)
National Oceanic and Atmospheric Administration (NOAA) – US [18]	This website maintains and provides access to data of databases of ASOS, AWOS, and METAR. Meteorological data in various formats (e.g., historical, statistical...)
Climatic Atlas of Clouds Over Land and Ocean [19]	Parameters that allow the characterisation of various cloud types, such as frequency of occurrence, base height...

II. DATA GATHERING

As introduced earlier, the atmospheric events are characterized for many parameters, most of the times not easy to find. In order to obtain them, including the visibility, some databases have been searched in different sources. The meteorological data collected from the sources of Table 1, is mainly obtained from the Automated Surface Observation System (ASOS), the Automated Weather Observation System (AWOS) or Meteorological Aerodrome Reports (METAR). Specifically, both ASOS/AWOS networks provide automated observations on an ongoing basis. As mentioned above, Table 1 shows the sources that have been consulted to obtain the parameters used in this paper.

III. THEORETICAL BACKGROUND

In this section, the parameter of visibility, in particular the daytime and nighttime visibility, and the atmospheric attenuation in FSOC is described in detail. In the case of visibility, the different procedures for calculating them are specified. The two values for the visibility are obtained in a different way. Regarding the FSOC attenuation sub-section, it describes the total atmospheric attenuation and the factors involved in it, such as the molecular and aerosol absorption and the molecular and aerosol scattering.

A. VISIBILITY

Visibility is presented as a fundamental parameter when calculating the attenuation by aerosol scattering in fog, but not only that. As mentioned before, this paper presents the idea of using it also in atmospheric events such as rain or snow. Due to the characteristics of FSOCs, a point-to-point communication with a necessary line of sight, the window of active communication in which a link can be established is variable as these events in each location are far from following a pattern. For this reason, for a complete analysis it is necessary to consider a day-time or night-time transmission, finding possible advantages depending on the link requirements and

resulting in exploring the characteristics of day and night visibility for the attenuation calculation.

The distance at which an object is distinguished from the background by the human eye is defined as visibility. In the case of daytime visibility, it is the distance at which an object is distinguishable with a certain threshold of background brightness [20] and in the case of nighttime visibility, with a known moderate light source [21]. The parameter of visibility is defined based on Koschmieder law as the distance of a light beam that is attenuated to a fraction of 2% or 5% of the original power [22]. It is evaluated at 550 nm, which is the wavelength that corresponds to the maximum intensity of the solar spectrum.

1) DAYTIME VISIBILITY

The daytime visibility (V_d) can be calculated as

$$V_d = \frac{-\ln \varepsilon}{\sigma} \tag{1}$$

where ϵ corresponds with the fraction of original power attenuated and σ is the extinction coefficient in km^{-1}. It is measured in km.

Koschmieder proposed a value of $\epsilon = 0.02$ in 1924 but the World Meteorological Organization proposed $\epsilon = 0.05$ to accomplish aeronautical requirements [23].

2) RELATIONSHIP BETWEEN DAYTIME AND NIGHTTIME VISIBILITY

This subsection presents the conventional way to calculate the night-time visibility based on the Allard law. In first place, the relation between the day-time and night-time visibility is presented, combining the Koschmieder and Allard law. Following with the explanation of calculating the night-time visibility with an iterative equation as it is done conventionally and proposing an alternative method with a simplified equation.

According to [20] and [24], combining the Koschmieder law and the Allard law in its simplified form, the relationship between daytime and nighttime visibility can be derived as

$$V_d = \frac{V_n \ln \varepsilon}{\ln(\frac{C_{\mathrm{DB}} V_n}{I_o})} \tag{2}$$

where

- I_o is the luminous intensity in lumens, whose value is 314.25.
- V_n is the nighttime visibility in km.
- σ is the extinction coefficient in km^{-1}.
- C_{DB} is the constant of proportionality in km^{-1}, whose value is 0.1351.
- V_d is the daytime visibility in km.

Hereafter, the equations for calculating the night-time visibility using the Allard law are explained, starting with (3) that shows the simplified form of Allard's law (in km).

$$e^{-\sigma V_n} = \frac{E_t V_n^2}{I_o} \tag{3}$$

It can be put it all in one term by equalling it to zero resulting in (4), where E_t is the visual threshold of illumination (Allard's law), which is $E_t = C_{DB}/V_n$.

$$V_n + \frac{1}{\sigma} \ln(\frac{E_t V_n^2}{I_o}) = 0 \tag{4}$$

We would like to point out that this equation is iterative and the visibility can not be calculated directly because it depends on the contribution of the rest of parameters. For this reason, Brent's iterative method [25] can be used to find a solution that satisfies the equation in order to obtain the visibility.

Figure 1 shows the comparison of both types of visibility. In ASOS networks, the procedure of distinguishing between the two types of visibility is already in use. The factors of this visibility comparison in km are shown below, which can be used to better characterize the time periods of nighttime and daytime for the main visibility thresholds in atmospheric events.

We propose to linearize Equation (2) as follows to avoid the iterative calculation in (4).

$$\begin{aligned} V_n &= V_d \cdot \varphi \\ \varphi &= 2.1, \quad V_d \leq 0.1km \\ \varphi &= 1.7, \quad 0.1 < V_d \leq 0.5km \\ \varphi &= 1.57, \quad 0.5 < V_d \leq 1km \\ \varphi &= 1.266, \quad 1 < V_d \leq 5km \end{aligned} \tag{5}$$

The threshold values have been selected according to the classification of fog depending on the visibility range shown later in section IV-A, specifically in Table 2. The reason for choosing this range is that fog is the most significant event in atmospheric attenuation for FSOC. Moreover, visibility under one kilometer is considered conditions of lower visibility. The first three cases correspond to the visibility ranges of dense, moderate and light fog, and the last one corresponds to the visibility range of haze/mist.

It can be seen in Figure 1 that under low visibility conditions (< 1 km) the curves are really similar, giving us the advantage of closer values in the worst case, while the error increases from 1km until it reaches 5km becoming almost equal. As mentioned before in the paragraph, the simplified form is used to avoid the use of the iterative equations, in which its calculations are not trivial.

B. ATMOSPHERIC ATTENUATION

Beers - Lambert law [26] describes the process where an optical beam is attenuated as it passes through the atmosphere. It is given by

$$\tau = e^{-\gamma L} \tag{6}$$

where τ is the value of the atmospheric transmittance,γ is the total atmospheric losses and L, the length of the optical link. In turn, the total atmospheric loss is made up of 4 different atmospheric loss values [1], which are:

$$\gamma = \alpha_m + \alpha_a + \beta_m + \beta_a \tag{7}$$

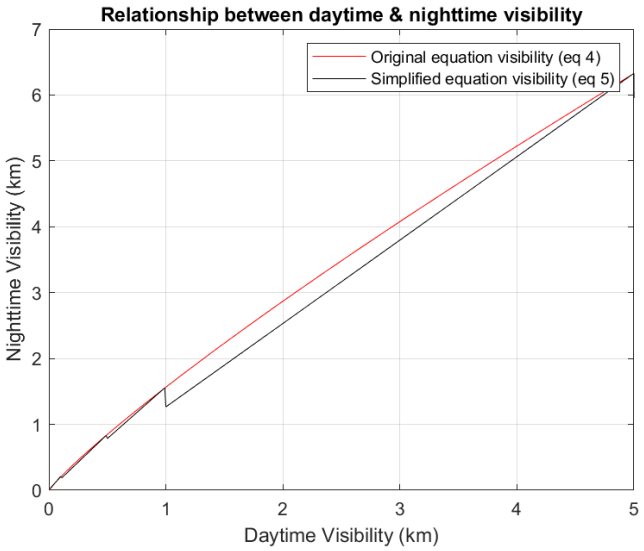

FIGURE 1. Error between Equation 4 (original) and Equation 5 (simplified form) of day/night time visibility.

- α_m is the attenuation of molecular absorption.
- α_a is the attenuation of aerosol absorption.
- β_m is the attenuation of molecular scattering.
- β_a is the attenuation of aerosol scattering.

As shown above, the atmospheric absorption and scattering attenuation consequently both split in molecular and aerosol atmospheric losses. In the visible and near infrared spectrum region [0.4μm – 2.4μm] the effects of absorption (both molecular and aerosol) and molecular scattering is negligible. In the first case, the imaginary part of the refractive index of these particles is really small and in the second case, the Rayleigh scattering phenomena is present and it is insignificant compared to Mie scattering [9].

IV. ATMOSPHERIC EVENTS IN FREE SPACE OPTICAL COMMUNICATIONS

As mentioned in the introduction, the atmospheric events are one of the challenges in the design of FSOC link and it is important to know the events that contribute most to the optical signal degradation. In this section, the features, types and the most relevant attenuation models of the main atmospheric events such as fog, rain, snow and clouds are presented.

A. FOG

Fog is defined as water droplets suspended in the atmosphere close to Earth's surface that affect visibility. As it was mentioned before, due to the fact that the fog particles size in the atmosphere are similar to the transmitter wavelength, the attenuation can be described by the Mie scattering theory. According to [26], for lower visibility the attenuation due to fog can reach 300 dB/km. Therefore, there is an important contribution of attenuation due to fog that must be considered in the design of FSOC. There are different types of fog depending on the visibility range. According to these criteria, in Table 2 the different types of fog are collected.

TABLE 2. Different types of fog depending on the visibility ranges.

Fog type	Visibility (km)	Comments
Dense fog	Visibility < 0.1	-
Moderate fog	Visibility ≈ 0.5	-
Light fog	0.5 < Visibility ≤ 0.9	-
Haze	1 < Visibility < 5	Considered Haze if relative humidity is below than 95%
Mist	1 < Visibility < 5	Considered Mist if relative humidity is greater than 95%
Clear	Visibility > 5	-

1) FOG ATTENUATION MODELS

In this subsection, it is described in detail the most commonly used attenuation models for fog, which is the most relevant atmospheric event in terms of attenuation contribution in the optical link.

a: KRUSE MODEL

Kruse model [1] has been used for modeling the fog for several years due to the dependency between the wavelength and the extinction coefficient. The extinction coefficient and the specific attenuation is given by (8) and (9) in km^{-1} and dB/km, respectively

$$\sigma = \frac{3.192}{V_d}\left(\frac{\lambda}{\lambda_0}\right)^{-q} \tag{8}$$

where λ is the wavelength and λ_0 is the wavelength reference used for visibility which is 550 nm.

$$\beta = n \cdot \sigma(\lambda) \tag{9}$$

n is a constant corresponds with $10 \log e$, equals to 4.34. The q parameter depends on the size distribution of the scattering particles, in this case is defined as:

$$\begin{aligned} q &= 0.585 V_d^{1/3}, \quad V_d < 6km \\ q &= 1.3, \quad 6 < V_d \leq 50km \\ q &= 1.6, \quad V_d > 50km \end{aligned}$$

b: KIM MODEL

Kim model [26] modifies the cases of lower visibility established by Kruse model, because apparently it was elaborated in conditions of light fog instead of dense fog conditions. Therefore, the wavelength-dependency is not considered in that scenario. In particular, the q parameter is the following:

$$\begin{aligned} q &= 0, \quad V_d < 0.5\ km \\ q &= V_d - 0.5, \quad 0.5 < V_d \leq 1\ km \\ q &= 0.16 V_d + 0.34, \quad 1 < V_d \leq 6\ km \\ q &= 1.3, \quad 6 < V_d \leq 50\ km \\ q &= 1.6, \quad V_d > 50\ km \end{aligned}$$

As it can be seen, Kim and Kruse models differs in parameter q.

c: AL NABOULSI MODEL

Al Naboulsi model [9] is based on the use of visibility as well, and it considers two types of attenuation for fog: advection and radiation. The operative wavelength is in the range of 690 to 1550 nm and the visibility range varies from 0.05 to 1 km. The Al Naboulsi model shows a wavelength dependence greater in radiation than advection. It pretends to correct the non accurate prediction of Kruse and Kim model of visibility lower than 500m. This problem arises because it does not differentiate between several types of atmosphere aerosols and distributions and propagation media. The definitions of advection and radiation mentioned in [21] are the following:

- Advection: movements of wet and warm air masses above the colder maritime and terrestrial surfaces.
- Radiation: related to ground cooling by radiation.

The extinction coefficient (km^{-1}) and the specific attenuation (dB/km) in this case is given by (10), (11) and (12):

$$\sigma_{adv} = \frac{0.11478 \cdot \lambda + 3.8367}{V_d} \tag{10}$$

$$\sigma_{rad} = \frac{0.18126 \cdot \lambda^2 + 0.13709 \cdot \lambda + 3.7502}{V_d} \tag{11}$$

$$\beta_{rad/adv} = n \cdot \sigma_{rad/adv} \tag{12}$$

d: FOG OPTIMIZATION MODELS

In [27], Nadeem et al. proposed an optimization model resulting in lower root-mean squared error (RMSE) values than previous models. Besides, in this paper, the data of the specific attenuation measured for 830 nm and 1550 nm in 2009 at the Czech Metrological Institute were used. Due to the behavior of the data and the fog models, a power law equation is chosen and also, from the coefficients for either the 830 nm case and the 1550 nm, a generic model with the following values has been derived.

$$\alpha_{Nadeem} = a \cdot e^{b \cdot V_d} + c \cdot e^{d \cdot V_d} \tag{13}$$

$$a(\lambda) = 185.8 - 0.0522 \cdot \lambda$$

$$b(\lambda) = -2.239 \cdot 10^{-6} - 0.002148 \cdot \lambda$$

$$c(\lambda) = 25.42 + 0.01869 \cdot \lambda$$

$$d(\lambda) = 0.0008465 - 7.41 \cdot 10^{-7} \cdot \lambda$$

The coefficients a, b, c and d above are wavelength-dependent and they are given in nanometers. A resume of the models are shown in Table 3.

B. RAIN

According to [1], the size of rain particles which are of the order of 100 to 10000 μm, which means that are way higher than the wavelength, therefore the rain attenuation is much lower than fog in FSOC. The rain attenuation can be calculated with the empirical techniques proposed by the ITU-R or physical methods such as the Marshall-Palmer model [28].

TABLE 3. Resume of the features of the fog models analyzed in section IV-A-I.

Model	Model Type	Wavelength (λ-nm)	Wavelength dependency
Kruse	Attenuation	[400–2400]	Wavelength dependency considered
Kim	Attenuation	[400–2400]	Wavelength dependency not considered at lower visibilities
Al Naboulsi	Attenuation	[690 – 1550]	Wavelength dependency considered

1) RAIN ATTENUATION MODELS

The specific attenuation of rain (dB/km) can be mainly calculated through the following power law equation:

$$\beta_{rain} = kR^{\alpha} \tag{14}$$

In (14) the parameter R is the rain precipitation rate in mm/h. The values of k and α depend on the rain particle size and composition and consequently it varies according to the model. In this case, to calculate the rain attenuation, there are several models that can be used to estimate the specific attenuation. They have been developed in different locations and under different conditions, so their behavior in certain sections is somewhat different. In particular, this document analyses the relations or models of Carbonneau, Japan and Marshall-Palmer.

a: CARBONNEAU RELATION

The Carbonneau relation is proposed by the ITU-R for FSOC links and has its origins in France. In contrast to the Japan relation, it is an empirical relationship of a temperate region. For this reason, it does not consider high rainfall intensity values.

$$k = 1.076$$
$$\alpha = 0.67$$

b: JAPAN RELATION

The Japan relation is the other rain model proposed by the ITU-R for FSOC links and has its origins in Japan. In this case, it is an empirical relationship of a tropical region.

$$k = 1.58$$
$$\alpha = 0.63$$

c: MARSHALL AND PALMER RELATION

The Marshall and Palmer relation is a physical relationship that is based on the Marshall and Palmer drop size distribution. During years, it has been a very common relationship to describe the attenuation of the rain intensity rate in a wide range of scenarios.

$$k = 0.365$$
$$\alpha = 0.63$$

TABLE 4. Resume of the features of the rain models analyzed in section IV-B-I.

Model type	Model name	Comments
Empirical	Carbonneau	Temperate region. It was elaborated from low rain intensity rates.
Empirical	Japan	Tropical region.
Physical	Marshall - Palmer	With low rain intensity rates the behavior is closer to Carbonneau/Japan model.

TABLE 5. Types of rain intensity depending on the rain intensity rate per hour.

Rain intensity rate per hour (mm/h)	Type of rain intensity
<1	Very mild
1-5	Mild
5-10	Moderate
10-20	Heavy
>20	Very heavy

As extracted from [28], there is a comparison between these models. It can be seen that in the Japan and Carbonneau relations, usually have higher values with respect to the measured values of the specific attenuation, in contrast to the Marshall and Palmer relation, that has lower values. In low rain intensity rates, all the models are really similar even though the rain intensity increases, the difference is more significant. Table 4 contains a resume of the different rain models and Table 5 contains the common rain intensity rate values.

C. SNOW

Snow is considered as frozen precipitated water falling to the ground. As the snow particles size are between fog and rain, their contribution to the atmospheric attenuation is way more than rain. In case of several/torrential snow intensity rates the attenuation could be similar to dense fog conditions.

There are two types of snow, wet snow for heights below 500m and dry snow for heights above 500m [1]. Wet snow is formed when temperatures are close or below to 0°C and contains 2 or 3 times more water content than dry snow, so this type of snow is denser. Temperatures below 0°C cause the appearance of dry snow, much lighter and with less water content [29].

1) SNOW ATTENUATION MODELS

The specific attenuation of snow can be calculated in the same way as rain:

$$\beta_{snow} = kS^{\alpha} \tag{15}$$

The parameter S is the snow precipitation rate in mm/h. Also, the parameters for each type of snow can be calculated as:

- Dry snow: $k = \lambda \cdot 5.42 \cdot 10^{-5} + 5.49,\ \alpha = 1.38$
- Wet snow: $k = \lambda \cdot 1.02 \cdot 10^{-4} + 3.78,\ \alpha = 0.72$

TABLE 6. Types of snow intensity depending on the rain intensity rate per hour.

Snow intensity rate ranges (mm/h)	Type of snow intensity	Mean values snow intensity rate range (mm/h)
2-15	Moderate	8
15-30	Strong	20
30 - 60	Several	45
>60	Torrential	65

In both equations, apparently, there is a wavelength dependency. It has to be said that it does not cause significant variations in the results so it can be considered negligible. In Table 6, the common snow intensity rate values and snow types are shown:

D. RELATIONSHIP BETWEEN THE PRECIPITATION RATE AND VISIBILITY

The rain attenuation models as well as the snow attenuation models depend on the precipitation intensity rate. In this section, the estimation of precipitation rate for rain and snow using the parameter of visibility, is derived.

1) RAIN

In the case of rain, according to [30], using the work from Stallabrass (1985) [31], and Marshall and Palmer (1948) [32], we can establish a relationship between the visibility and the rain intensity rate.

- The Stallabrass equation relates the specific attenuation and the Liquid Water Content (LWC). The LWC describes the amount of condensed water in g/m3.

$$\beta_{Stallabrass} = 2.24 \cdot \mathrm{LWC}^{0.75} \tag{16}$$

- Marshall and Palmer established a LWC distribution of rain that depends on the precipitation intensity rate of rain, that is, the amount of rain that would fall in a time interval if the amount of rainfall were assumed to be constant during that time. As can be seen in (17), R is the rain intensity rate in mm/h.

$$\mathrm{LWC}_{Marshall-Palmer} = 0.072 \cdot R^{0.88} \tag{17}$$

- Koschmieder law (1) that relates the visibility and the specific attenuation mentioned in section III-A-I.

Therefore, a relationship between visibility and the rain precipitation rate is given by (18), in which the parameter V_d is the daytime visibility in km.

$$R = 42.84 \cdot \left(\frac{1}{V_d}\right)^{1.438} \tag{18}$$

2) SNOW

In the case of snow, according to [20], there are two parametrizations in the case of dry and wet snow, given

TABLE 7. Parameter values of eq. 17, eq.18, obtained from.

Parameters	Dry snow	Wet snow
V_t	0.017	0.072
C_3	100	200

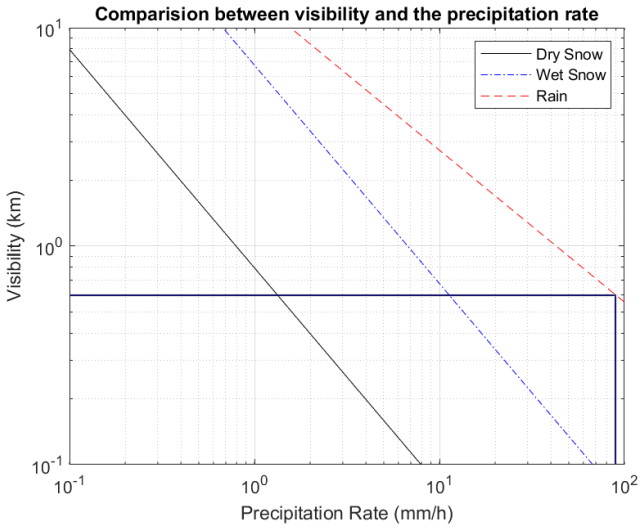

FIGURE 2. Comparison between the visibility and the precipitation rate.

by (19), (20):

$$S = \frac{0.36 \cdot \delta}{V_d} \tag{19}$$

$$\delta = 1.3 \cdot C_3 \cdot V_t \tag{20}$$

- V_t is the terminal velocity in $\frac{cm}{s}$
- C_3 is a constant with different values for dry or wet snow in $\frac{g}{cm^2}$
- V_d is the daytime visibility in km
- S is the precipitation rate in $\frac{mm}{h}$

The values of C_3 and V_t for each type of snow are the following:

Figure 2 shows the relationship between visibility and the precipitation rate for dry snow, wet snow and rain. The dark blue line marks the rain intensity rate limit, which 90 mm/h corresponds to a torrential tropical rain and it is associated with a 0.6 km of visibility. It is clear that rain has a lower effect on visibility than snow. On the other hand, at the same precipitation rate, dry snow is more significant in terms of visibility than wet snow, therefore it can reach higher attenuation values.

E. CLOUDS

Another atmospheric event that can increase the attenuation into the optical signal are clouds. The cloud attenuation is mainly caused by airborne particles such as aerosols or water droplets. Transmitting an optical signal through clouds could affect the link availability, so it has also to be considered to envisage the most realistic FSOC scenario.

TABLE 8. Parameters of different cloud types.

Cloud classification	Cloud type name	Typical base height (km)	Vertical extension (km)
High Clouds	Cirrus	6 - 10	1.0-2.5
Middle Clouds	Cumulus	0.5 - 1.0	0.5-5
Middle Clouds	Altostratus	2 - 6	0.2-2
Middle Clouds	Nimbostratus	0.1 - 1.0	2-3
Low Clouds	Stratocumulus	0.6 - 1.5	0.2-0.8
Low Clouds	Stratus	0.1 - 0.7	0.2-0.8

TABLE 9. Cloud heights for low, mid and high clouds.

Types of clouds	Cloud height (km)
Low Clouds	< 2
Middle Clouds	2 - 6
High Clouds	> 6

Depending on the type of clouds, the specific attenuation (dB/km) may vary from dozens to hundreds and could result in an optical link outage. In general, lower and middle clouds add similar attenuation as dense fog conditions, thus a blockage. In the case of high clouds such as cirrus, the attenuation is much lower so it is interesting to calculate the specific attenuation in this situation. However, in terms of cloud attenuation, it is worth to calculate the percentage of cloud blocking depending on the location. In this section, methods for estimating the cloud attenuation and the percentage of cloud blocking are presented.

Depending on the height of such clouds, these can be classified into high, middle, and low clouds [33]. In Table 8 it can be seen a resume of some cloud types, their typical base height and extension in km, and in Table 9, the cloud heights of the general types of clouds.

1) CLOUD ATTENUATION MODELS

There are various methods to calculate cloud attenuation. In [34] some methods for calculating cloud attenuation are presented. Let's summarize the main ones in the following.

a: MODEL BASED ON MIE SCATTERING THEORY

Particularly, in this case, cloud droplets are considered spherical and small in size. This model estimates the cloud attenuation based on the elevation angle and the height of an Optical Ground Station (OGS). The elevation angles have to be around 45° and the height of the ground station between 0 and 5 km. It is given by (21), in which A_{cloud} is the cloud attenuation in dB, θ is the elevation angle of the optical ground station in degrees and σ is the extinction coefficient in km^{-1}:

$$A_{cloud} = \frac{n \cdot \sigma}{\sin\theta} \tag{21}$$

As mentioned before, n is a constant with value 4.34 ($\log e$) and the extinction coefficient is equivalent to the following:

$$\sigma = a' \cdot h_{gs}^3 + b' \cdot h_{gs}^2 + c' \cdot h_{gs} + d' \tag{22}$$

- h_{gs} is the height of the ground station in m.

TABLE 10. LWC of different cloud types.

Cloud Classification	Cloud type name	LWC ($\frac{g}{m^3}$)
High Clouds	Cirrus	0.03
Middle Clouds	Cumulus	0.26
Low Clouds	Stratocumulus	0.44
Low Clouds	Stratus	0.28
Low Clouds	Cumulonimbus	1 - 3

- a', b', c', d' are parameters which have wavelength dependency.

$$a'(\lambda) = -0.000545 \cdot \lambda^2 + 0.002 \cdot \lambda - 0.0038$$
$$b'(\lambda) = -0.00628 \cdot \lambda^2 - 0.0232 \cdot \lambda - 0.0439$$
$$c'(\lambda) = -0.028 \cdot \lambda^2 + 0.101 \cdot \lambda - 0.18$$
$$d'(\lambda) = -0.228 \cdot \lambda^3 + 0.922 \cdot \lambda^2 - 1.26 \cdot \lambda + 0.719$$

b: ATTENUATION CALCULATION BASED ON THE RELATION BETWEEN THE LWC AND VISIBILITY

In this section, two forms of estimating the visibility using the LWC, which is a common parameter of clouds, are presented. These standard LWC values for different types of clouds and other parameters such as the frequency of occurrence, that helps to characterize different locations are shown as well.

$$V_d = a \cdot \text{LWC}^b \tag{23}$$

Equation (23) uses only the LWC and two physical parameters a and b. These parameters are empirical constants if the default radiance were raised to daylight and their values are in the next range:

$$65 < a < 178$$
$$0.63 < b < 0.96$$

However, in (24) the visibility is estimated with the LWC and the cloud number concentration (N).

$$V_d = \frac{1.002}{(LWC \cdot N)^{0.6473}} \tag{24}$$

Due to the fact that the complexity to obtain this parameter is high, the standard LWC values of different cloud types are presented in Table 10 [35].

As mentioned in the previous section, the specific attenuation due to clouds can be calculated with the Kruse or Kim model used in fog conditions. Without a real measure of the LWC parameter, the standard values of LWC can be used depending on which type of cloud is at the moment. Knowing which type of cloud is in the path of the optical link is a difficult task, because not only one type of cloud could be in that instant, even 2 or more different clouds can be overlapped. In [36], depending on the latitude and length, if it is day, or night there are different statistical data about the frequency of occurrence of different types of clouds.

In [19] data such as the frequency of occurrence, amount of clouds and other parameters are collected from several years, and can be used as a template, which allows to know better

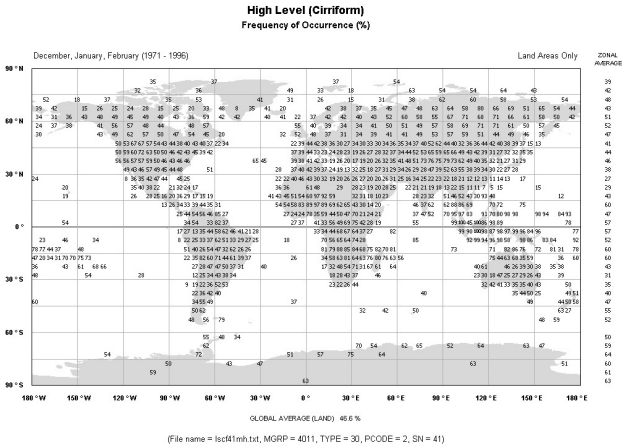

FIGURE 3. Average daytime/nighttime land cloud frequency occurrence of high levels clouds in 1971-1996 period [19].

TABLE 11. Meteorological parameters collected from the database in a CSV file.

Station Code	Date	skyl1	skyl2	skyl3
BIRK	01/01/2021 0:00	500.00	800.00	M
BIRK	01/01/2021 1:00	500.00	M	M
BIRK	01/01/2021 2:00	500.00	M	M
BIRK	01/01/2021 3:00	500.00	800.00	M
BIRK	01/01/2021 4:00	500.00	900.00	M
BIRK	01/01/2021 5:00	500.00	900.00	M

which type of cloud could be more likely to attenuate the optical path in a specific location. For example, for high level clouds, the frequency of occurrence average (day and night) between 1971 and 1996 is shown in Figure 3.

2) CLOUD SPECIFIC ATTENUATION METHOD

From [16], the base length of clouds can be obtained from the columns "skyl1", "skyl2", "skyl3" for three different levels respectively. The 'M' code that appears in some column means that the values in that time instant for a specific level are missing. The CSV file is shown in Table 11.

In a similar way as mentioned in [34], the vertical path where the different types of clouds are, can be divided in layers and calculate the specific attenuation of each one with their corresponding width. An example can be seen in Figure 4. If the base height data from the database and this layer structure is combined, it can be determined which cloud type is more probable to be in each layer and a time instant and calculate the specific attenuation.

With this parameter, the specific attenuation is calculated for the most likely cloud type at each layer. Then, with the vertical extension of each cloud type the total attenuation of each path can be calculated as well.

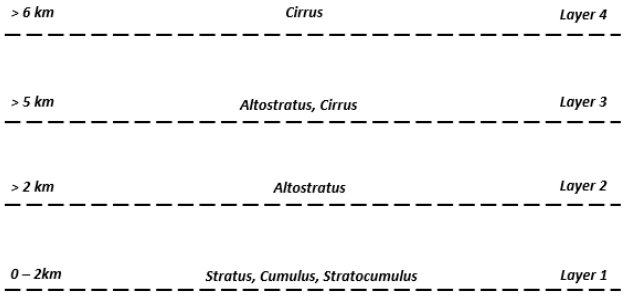

FIGURE 4. Example of a layer structure used in the cloud attenuation calculation.

TABLE 12. METAR codes and oktas associated.

Cloud Blockage METAR code	Name	Oktas	Description
CLR	Sky clear	0/8	No cloud cover detected under 12000 ft (3.6576km)
FEW	Few clouds	1/8 , 2/8	It can be considered as almost clear
SCT	Scattered	3/8 , 4/8	-
BKN	Broken	5/8 , 7/8	-
OVC	Overcast	8/8	Total cloud cover

3) CLOUD BLOCKAGE PERCENTAGE CALCULATION METHOD

In [16], the METAR parameter called "Cloud Coverage Level" is reported as well. It is a METAR code used in airports to give information about the cloud coverage of the sky. The sky over the meteorological station is partitioned in eight equal parts called oktas. For example, if an okta is detected and reported, it means that 1/8 of the sky is covered by clouds. There are different METAR codes depending on how many oktas are detected and reported by the meteorological station and it can be seen in Table 12.

These meteorological codes can be used to note the percentage of the sky that is covered by clouds during a period of time and it can help to estimate the percentage of cloud blockage in a specific location, which can result in a link outage.

V. RESULTS AND DISCUSSION

After the theoretical section of each atmospheric event and the developed relationship between some of them, the results have been analysed to explain the behavior of some of the models in detail.In this section, analyses and calculations are carried out on the estimation of fog specific attenuation and the cloud blockage probability. An explanation of the method to calculate the cloud specific attenuation and the relationship of the attenuation of fog, rain and snow based on a common a parameter (visibility) are also included here. It is to be said that, both visibilities (day-time and night-time) can be used on the methods, and the choice depends on the situation and scenario.

TABLE 13. Parameters of the meteorological station in Canberra, Australia.

Location	Station Code	Parameter	Time Period
Canberra, Australia	YSCB	Visibility	[1-01-2022,9-01-2022]

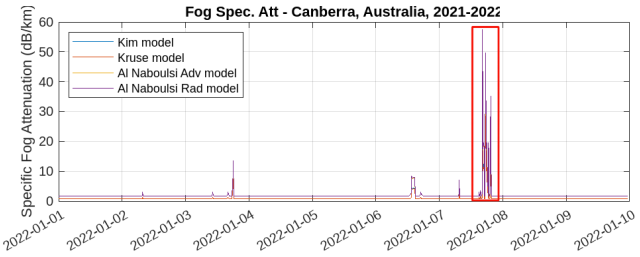

FIGURE 5. Specific attenuation due to fog. Canberra, 2-9/01/2022.

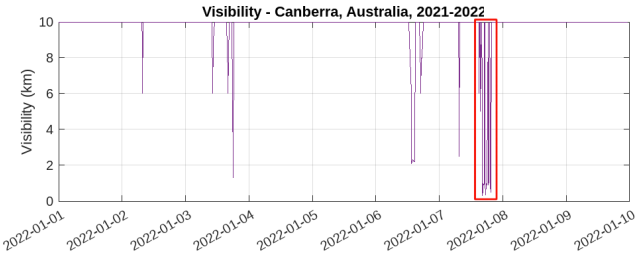

FIGURE 6. Visibility due to fog. Canberra, 2-9/01/2022.

A. FOG SPECIFIC ATTENUATION

The calculations of the fog specific attenuation have been done according to the following data and at two operation wavelengths: 1550 nm and 950 nm. Figure 5 and Figure 6 shows the specific attenuation calculated at 1550nm for the different fog models and the visibility during the first nine days of 2022 in Canberra. Table 13 shows the input information of the meteorological station.

As it can be seen in these figures, a low visibility event with a peak of 0.2 km from 14:24 to 19:12 on 7 January has been highlighted in a red box. In this event, the specific attenuation reaches more than 50 dB/km. It is due that in Canberra at that time there was a moderate - dense fog conditions.

1) COMPARISON OF THE DENSE FOG EVENT FOR TWO OPERATIVE WAVELENGTHS

In order to check the effect of the wavelength, the fog event on 7 of January previously mentioned is selected for the analysis of the fog models. Those results are drawn in Figure 7 and 8.

From this figure, several conclusions can be obtained. First of all, for lower visibility values the Kruse and Kim model have a worse performance than the Al Naboulsi model. Another important observation that can be extracted from this figure is that dependency with frequency of the attenuation is not always the same and moreover, it could even be independent. For example, in the case of Kim model, below 500m

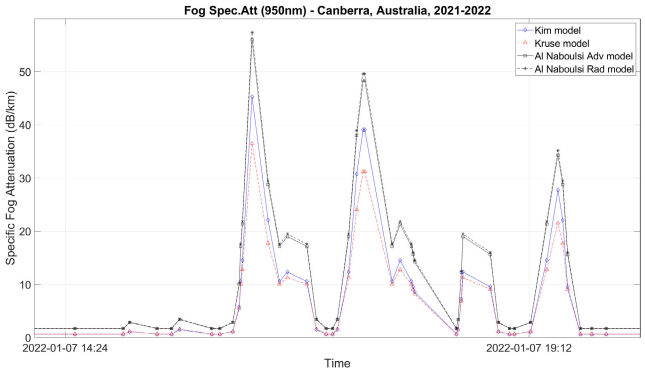

FIGURE 7. Specific attenuation of the fog event at 950 nm on 7 of January.

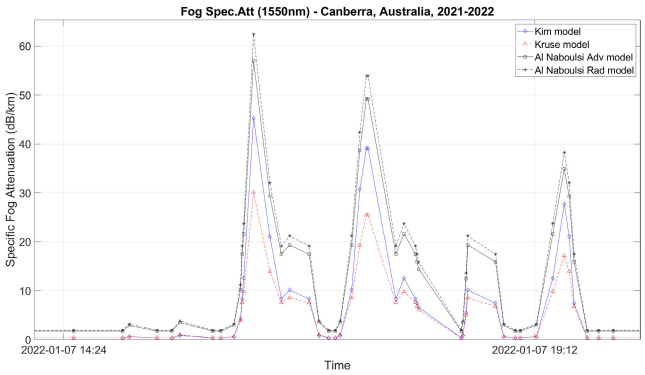

FIGURE 8. Specific attenuation of the fog event at 1550 nm on 7 of January.

of visibility, for q=0 there is no dependency with wavelength since both values are the same (950 and 1550 nm). In contrast, the Kruse model attenuation increases in the 950 nm compared to 1550 nm case. As the visibility values increase, the differences between Kruse and Kim models become smaller. On the other hand, it can be seen the Al Naboulsi wavelength dependency in the specific attenuation when the wavelength increases. This behavior occurs because it is directly proportional to the wavelength (in the case of radiation is directly proportional to the square of the wavelength) which results in an attenuation drop when the wavelength decreases. Thus, the wavelength dependency in Al Naboulsi implies a greater attenuation for higher wavelength, and for the Kruse model, a greater attenuation with lower wavelength, what proofs our explanations.

B. CLOUDS

The calculations of the cloud specific attenuation and the link probability blockage have been performed according to the following locations. The station code, time period and coordinates are given in Table 14.

1) CLOUD SPECIFIC ATTENUATION CALCULATION

For two locations, namely, Canberra and Reykjávik, the average data collected of the frequency of occurrence for different

TABLE 14. Meteorological parameters in several locations.

Location	Parameter	Time Period	Latitude	Longitude
Canberra, Australia	YSCB	[2020-2022]	35°18'32"S	149°12'1"E
Reykjavík, Iceland	BIRK	[2020-2022]	64°7'42"N	21°56'27"W
Tenerife, Spain	GCXO	[2020-2022]	28°28'59"N	16°20'32"W
Oslo, Norway	ENFB	[2020-2022]	61°12'22"N	1°49'45"E
Honolulu, Hawaii	PHNL	[2020-2022]	21°19'39"N	157°56'35"W
Atacama, Chile	SCAT	[2020-2022]	27°15'44"S	70°46'26"W
Tokio, Japan	RJAA	[2020-2022]	35°45'55"N	140°23'8"E

TABLE 15. Average frequency of occurrence data in Canberra from 1971 to 1996.

Cloud type	Frequency of occurrence
Stratus	9%
Cumulus	29%
Stratocumulus	34%
Cirrus	43%
Altostratus	7%
Cumulonimbus	5%

TABLE 16. Average frequency of occurrence data in Reykjávik from 1971 to 1996.

Cloud type	Frequency of occurrence
Stratus	21%
Cumulus	10%
Stratocumulus	45%
Cirrus	40%
Altostratus	25%
Cumulonimbus	16%

cloud types in the time period of 1971-1996 is shown in Table 15 and Table 16.

According to the layer diagram mentioned in section IV-E-II, in case the cloud height matches a layer with two or more types of clouds, the frequency of occurrence is used to select the LWC of the most probable type of cloud in the selected location. Using (23) to calculate the visibility and then (8), the specific attenuation of the cloud can be obtained. Afterwards, the total attenuation can be calculated by multiplying the specific attenuation with the average length extension of the cloud type, where the typical cloud extension can be found in Table 8. Even though this is a good method to calculate the total attenuation of clouds specifically, it does not give us any useful information because the attenuation is very high (in the order of hundreds of dB/km of attenuation) that it probably causes a fading of the link.

2) PROBABILITY OF LINK BLOCKAGE

However, the time that an OGS can be available to establish an optical link is essential and it could be really helpful for near-Earth or deep space missions. As it is mentioned in section IV-E, the presence of clouds over the OGS causes

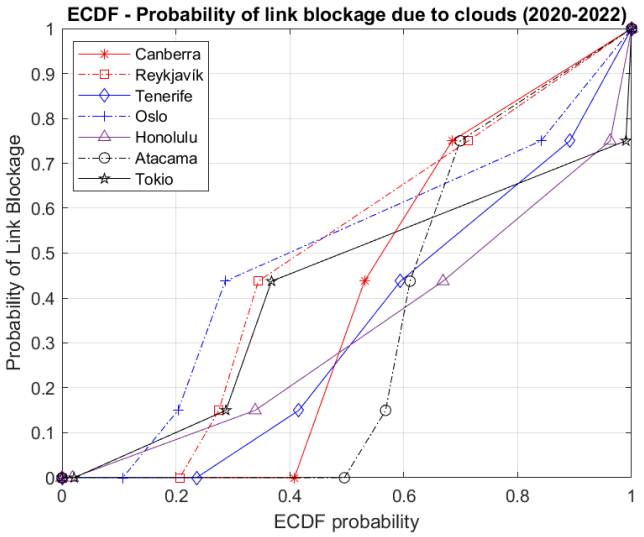

FIGURE 9. CDF of the probability of link blockage for several locations during the period 2020 - 2022.

hundreds of dB/km and can result in link blockage. For this reason, it is assumed that the presence of clouds results in a blockage of the link. The probability of link blockage for the locations of Table 14 during a period of 2 years is shown in Figure 9.

In Figure 9, the CDF of the probability of link blockage that can result in a non available link is shown for different locations. As it can be seen in the figure, curves that follow the same trend are given for locations with closer latitudes, such as Reykjávik - Oslo, or Tenerife - Honolulu. Following these results, it is clear that Tenerife and Honolulu are a better choice to establish an optical link between an OGS and a satellite, because the percentage of time that the link can be blocked by clouds is around 50%. For example, at 70%, there is a 47% and 55% or less of link blockage at Honolulu and Tenerife respectively, whereas there is a minimum of 60% (at Tokio) up to almost 80% in the rest of locations. Of course, these results are obtained for a period of 2 years, and it would be more accurate with a more extensive time period or instead of considering the whole year, just for certain seasons when the data is going to be used.

3) FOG, SNOW AND RAIN ATTENUATION BASED ON VISIBILITY

In this section, the usage of fog, rain and snow models based on the visibility parameter is analyzed. The models that have been used for this approach are shown in Table 17.

A comparison of the specific attenuation curves of fog, rain and snow is given in Figure 10. The dark blue line matches the rain intensity rate limit. As can be seen in drastic visibility conditions, fog attenuates more than snow. However, in case of heavy snow conditions the attenuation values are of the same order as fog. On the other hand, rain has lower values of attenuation than fog and snow. For example, the blue line matches the visibility (0.6 km) due to a rain intensity rate

TABLE 17. Information about the atmospheric events models and features used in section IV-B.

Atmospheric events	Model	Comments
Fog	Kim	Evaluated with a λ = 1550 nm
Snow	Dry/Wet snow	Mean values of dry and wet snow parameters.
Rain	Marshall and Palmer parameters	Procedure followed in section D-1

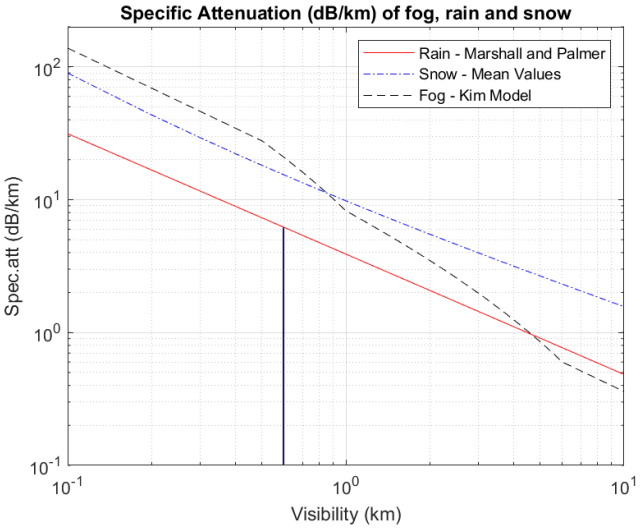

FIGURE 10. Comparison of the specific attenuation curves of fog, rain and snow.

of 90 mm/h, that corresponds to a torrential tropical rain, which is not reached in temperate regions and it implies a specific attenuation of 6 dB/km. As we move further away in visibility, the specific attenuation values decrease for snow and fog, reaching 6 dB/km for visibility of almost 2 km in case of snow, and 1.5 km in case of fog. Therefore, it can be stated that only in the case of really improbable situations in the case of rain (and somewhat less for snow) for very low visibility, the attenuation values can be at the level of fog.

Besides, in the rain case we analyzed the variations between the model chosen (Marshall-Palmer) with either the Carbonneau and the Japan model. It is shown in Figure 11, where the biggest difference is located in low visibility conditions (visibility < 0.5 km) but as we already commented in section IV-D, this is not realistic because it suposes an exorbitant precipitation rate in the relation with the visibility. Therefore, if we consider the visibility from 0.67 km and so on, the variation between the Marshall – Palmer model and Carbonneau/Japan decreases from almost 15 dB to 3 dB (considering the Japan model as the worst case). Finally, in the case of the snow attenuation models that it is shown in Figure 12, we considered the average values of the wet and dry snow so the curves are simmetrical. Thus, the biggest variation is located again in very low visibility conditions, but it is more useful to look at it from 0.25 km to 4km, where the precipitation rate has typical values and so the visibility for

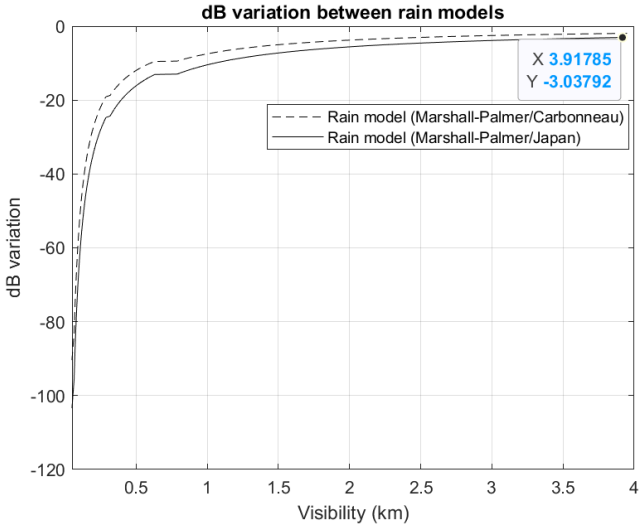

FIGURE 11. Analysis of the variation of the rain attenuation models.

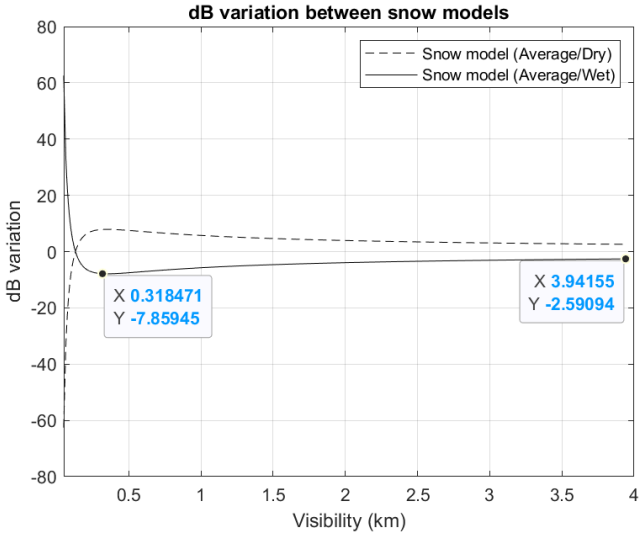

FIGURE 12. Analysis of the variation of the snow attenuation models.

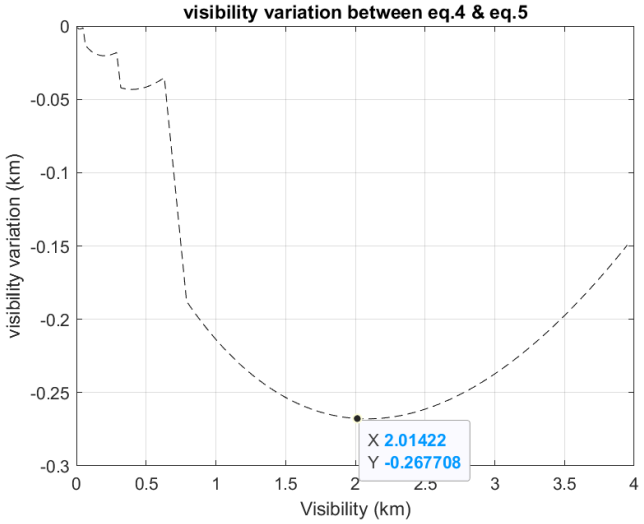

FIGURE 13. Analysis of the variation of the visibility day-night time equations 4-5.

the snow. In this interval, a variation from 7.9 to almost 2.6 dB can be seen.

It is shown the variation between (5) and (4) in Figure 13, that corresponds to the simplified form of the day/night time visibility and the original form. In the low visibility interval ($0<V<1$ km), where is more interesting for the analysis, the variation is quite small with an average of 0.1 km and as we go through higher visibility values we end up at a maximum of 0.26 km aproximately. Later on, the variation decreases to 0.15 km.

We can conclude that in the rain case, we find the higher values and we can not ignore than a maximum difference of 12 dB is considerable when designing a communication system. Besides, with higher values of visibility that corresponds with more realistic precipitation rate values, the error is lower. It is true, however, that for a specific system design, those models that have been made for specific environments should be chosen, as they will be more accurate because we have gone for a conservative approach. However, as the purpose of this paper is to propose an analysis method at a system level with a special focus of characterizing multiple locations, this variations can be considered as a mitigation margin that has been underestimated, as the rain and the snow are the atmospheric events that has less impact on FSOC links, and we are not strictly designing a system. Concerning the snow case, we came to a similar conclusion as with the case of rain even though the variations are smaller. To conclude, we think that in the case of the proposed simplified equation of the day/night time visibility and the original, is quite usable. The variations are not significant and it allows us to calculate both visibilities easier than with the original case. As a final note, we think that these variations have to be taken into account in order to make a complete analysis for several locations.

As in these models the visibility parameter is used, a general expression for the specific attenuation (dB/km) due to aerosol scattering that includes these three events could be given by (25).

The fog atmospheric attenuation term can be expressed by (8) in which we choose the q values of the Kim model in section IV-A-b considering its operation distance, which extends to several km and its correction in dense visibility conditions with respect to Kruse model. On the other hand, the rain atmospheric attenuation term can be expressed using (18) in (14). We consider the use of Marshall and Palmer parameters, that as a physical relationship, is commonly used to relate the liquid water content of several rain intensity rates based on the rain particle size distribution. As mentioned in section IV-B, the behavior of the rain attenuation models are really similar in low rain intensity rates, but they differ as it increases the rain intensity rate. Therefore, we have opted for a conservative model that could be valid

for different scenarios because the work behind this paper pretends to characterize multiple locations. Finally, the snow atmospheric attenuation term can be expressed using (19) in (15) and considering the mean values of both the dry and wet snow, as it is complicated to determinate the snow type in different locations. The integration of the fog, rain and snow models discussed above into a single visibility-based model makes it easier to characterise the attenuation of these events. One aspect to highlight is the possible loss of precision in the calculations due to the fact that, as our objective is to characterise a multitude of locations, generic and conservative models have been chosen with respect to models that can characterise a specific region, in order to give more versatility to the results.

$$\beta_{atm}(Vis) = \beta_{fog}(Vis) + \beta_{snow}(Vis) + \beta_{rain}(Vis) \qquad (25)$$

VI. CONCLUSION

This paper presents the main atmospheric events that most affect the free-space optical links. Those parameters can be present in different link configurations. Besides, a single parameter (visibility) has been developed to establish relationships for all the events. The visibility is easier to obtain for all the community and that allows to carry out appropriate estimations. The sources in which the meteorological parameters have been obtained are also in section II.

A theoretical background about daytime, night-time visibility, and a brief introduction to total atmospheric losses is provided. On the other hand, fog, rain and snow have been analyzed on the basis of visibility, giving their main characteristics, providing the most common attenuation models that have been used for each of them. They have been analyzed and explained. Regarding the clouds, which are a meteorological phenomenon that can be said with some certainty to be frequently present in free-space optical communications between satellites and the OGS, they have also been related to visibility, showing several methods for calculating attenuation considering the type of clouds. Also using aviation METAR codes, a new method for estimating the probability of cloud presence is presented.

Finally, various analysis have been carried out, such as the different fog attenuation models, the link blockage probability calculations using the latest mentioned method, and the behavior of the specific attenuation of fog, snow and rain have been analyzed as a whole. As for the probability of link blockage, data from 7 locations have been used: Canberra, Reykjavik, Tenerife, Honolulu, Atacama, Oslo and Tokyo, where some of them already have astronomical stations and observatories, showing Tenerife and Honolulu as the best options for the location of OGS. It should be mentioned that the method can be improved by discriminating for specific time periods such as certain seasons for various locations, and it is useful to recognise trends, using cloud coverage codes reported from the same sources as visibility. On the other hand, regarding the specific attenuation of fog, rain and snow, it is clear that fog makes the most important contribution followed by snow and rain, and, although at very small visibility values, snow and even rain may have the behavior of fog attenuation curves. This means having very adverse atmospheric conditions that may only occur in certain locations, compared to moderate to high fogs in many parts of the world. Thus, it can be concluded that, the selection of the location for the OGS is important but also there are several good candidates for their locations.

REFERENCES

[1] H. Kaushal and G. Kaddoum, "Optical communication in space: Challenges and mitigation techniques," *IEEE Commun. Surveys Tuts.*, vol. 19, no. 1, pp. 57–96, 1st Quart., 2017.
[2] M. Z. Chowdhury, M. K. Hasan, Md. Shahjalal, E. B. Shin, and Y. M. Jang, "Opportunities of optical spectrum for future wireless communications," in *Proc. Int. Conf. Artif. Intell. Inf. Commun. (ICAIIC)*, Feb. 2019, pp. 4–7.
[3] T. Yamazato, N. Kawagita, H. Okada, T. Fujii, T. Yendo, S. Arai, and K. Kamakura, "The uplink visible light communication beacon system for universal traffic management," *IEEE Access*, vol. 5, pp. 22282–22290, 2017.
[4] A. S. Ghazy, H. S. Khallaf, S. Hranilovic, and M. Khalighi, "Undersea ice diffusing optical communications," *IEEE Access*, vol. 9, pp. 159652–159671, 2021.
[5] E. Leitgeb, "Future applications of optical wireless and combination scenarios with RF technology," in *Proc. 40th Int. Conv. Inf. Commun. Technol., Electron. Microelectron. (MIPRO)*, May 2017, pp. 404–406.
[6] E. Leitgeb, T. Plank, P. Pezzei, D. Kraus, and J. Poliak, "Integration of FSO in local area networks-combination of optical wireless with WLAN and DVB-T for last mile internet connections," in *Proc. 19th Eur. Conf. Netw. Opt. Commun. (NoC)*, Jun. 2014, pp. 120–125.
[7] M. Z. M. Khan, "Towards InAs/InP quantum-dash laser-based ultra-high capacity heterogeneous optical networks: A review," *IEEE Access*, vol. 10, pp. 9960–9988, 2022.
[8] *National Aeronautics and Space Administration (NASA)*. Accessed: Oct. 8, 2022. [Online]. Available: https://www.nasa.gov/directorates/heo/scan/opticalcommunications/timeline
[9] M. C. Al Naboulsi, F. De Fornel, H. Sizun, M. Gebhart, E. Leitgeb, S. S. Muhammad, B. Flecker, and C. Chlestil, "Measured and predicted light attenuation in dense coastal upslope fog at 650, 850, and 950 nm for free-space optics applications," *Opt. Eng.*, vol. 47, no. 3, 2008, Art. no. 036001.
[10] M. K. Alfalih, I. Myderrizi, A. Solyman, and M. Mohammed, "Effects of Istanbul's weather on free-space optical communications," in *Proc. Int. Symp. Multidisciplinary Stud. Innov. Technol. (ISMSIT)*, Oct. 2022, pp. 251–256.
[11] S. Sugumaran, G. Sampath, G. Deivasikamani, N. K. Maurya, and C. V. V. S. Srinivas, "FSO (free space optics) application for various weather conditions and wavelengths," in *Proc. IEEE 2nd Mysore Sub Sect. Int. Conf. (MysuruCon)*, Oct. 2022, pp. 1–6.
[12] I. Hassan and A. Mandpura, "Free space optical communication system: Impact of weather conditions," in *Proc. Int. Conf. Signal Inf. Process. (IConSIP)*, Aug. 2022, pp. 1–5.
[13] A. Djir, F. Meskine, and M. L. Tayebi, "Free space optical communication study for image transmission under foggy conditions," in *Proc. 2nd Int. Conf. Adv. Electr. Eng. (ICAEE)*, Oct. 2022, pp. 1–6.
[14] O. A. Layioye, T. J. Afullo, P. A. Owolawi, and J. S. Ojo, "Effect of visibility variation on free space optical communication system over the eastern coast of South Africa using climatic data," in *Proc. 9th Int. Conf. Electr. Electron. Eng. (ICEEE)*, Mar. 2022, pp. 133–140.
[15] R. Nebuloni and E. Verdugo, "FSO path loss model based on the visibility," *IEEE Photon. J.*, vol. 14, no. 2, pp. 1–9, Apr. 2022.
[16] *Iowa State University*. Accessed: Oct. 8, 2022. [Online]. Available: https://mesonet.agron.iastate.edu/
[17] *Agencia Estatal de Meteorología (AEMET)*. Accessed: Oct. 8, 2022. [Online]. Available: https://www.aemet.es/
[18] *National Oceanic and Atmospheric Administration (NOAA)*.Accessed: Oct. 8, 2022. [Online]. Available: https://www.noaa.gov/
[19] R. Eastman and S. G. Warren. *Climatic Atlas of Clouds Over Land and Ocean*. Accessed: Oct. 8, 2022. [Online]. Available: https://atmos.uw.edu/CloudMap/

[20] R. M. Rasmussen, J. Vivekanandan, J. Cole, B. Myers, and C. Masters, "The estimation of snowfall rate using visibility," *J. Appl. Meteorol.*, vol. 38, no. 10, pp. 1542–1563, Oct. 1999.
[21] *American Meteorological Society (AMS)*. Accessed: Oct. 8, 2022. [Online]. Available: https://glossary.ametsoc.org/wiki/Fog
[22] M. Grabner and V. Kvicera, "The wavelength dependent model of extinction in fog and haze for free space optical communication," *Opt. Exp.*, vol. 19, no. 4, pp. 3379–3386, Feb. 2011.
[23] A. Prokes, "Atmospheric effects on availability of free space optics systems," *Opt. Eng.*, vol. 48, no. 6, Jun. 2009, Art. no. 066001.
[24] *Introduction to Atmospheric Visibility Estimation. Bristol Industrial and Research Associates Limited (BIRAL)*. Accessed: Mar. 6, 2023. [Online]. Available: http://www.biral.com/
[25] R. P. Brent, *Algorithms for Minimization Without Derivatives*. Englewood Cliffs, NJ, USA: Prentice-Hall, 1973.
[26] I. I. Kim, B. McArthur, and E. J. Korevaar, "Comparison of laser beam propagation at 785 nm and 1550 nm in fog and haze for optical wireless communications," *Proc. SPIE*, vol. 4214, pp. 26–37, Feb. 2001.
[27] F. Nadeem, T. Javornik, E. Leitgeb, V. Kvicera, and G. Kandus, "Continental fog attenuation empirical relationship from measured visibility data," *Radioengineering*, vol. 19, no. 4, pp. 596–600, 2010.
[28] A. Z. Suriza, I. Md Rafiqul, A. K. Wajdi, and A. W. Naji, "Proposed parameters of specific rain attenuation prediction for free space optics link operating in tropical region," *J. Atmos. Solar-Terr. Phys.*, vol. 94, pp. 93–99, Mar. 2013.
[29] M. Jessica. *NASA Snow Campaign Wraps 2020 Survey*. Accessed: Oct. 8, 2022. [Online]. Available: https://www.nasa.gov/feature/goddard/2020/nasa-snow-campaign-wraps-2020-survey
[30] I. Gultepe and J. A. Milbrandt, "Probabilistic parameterizations of visibility using observations of rain precipitation rate, relative humidity, and visibility," *J. Appl. Meteorol. Climatol.*, vol. 49, no. 1, pp. 36–46, Jan. 2010.
[31] J. R. Stallabrass, "Measurements of the concentration of falling snow," Snow Property Meas. Workshop, Nat. Res. Council Canada, LakeLouise, AB, Canada, Tech. Memorandum 140, 1985.
[32] J. S. Marshall and W. M. Palmer, "The distribution of raindrops with size," *J. Meteorol.*, vol. 5, pp. 165–166, 1948.
[33] K. Rammprasath and S. Prince, "Analyzing the cloud attenuation on the performance of free space optical communication," in *Proc. Int. Conf. Commun. Signal Process.*, Apr. 2013, pp. 791–794.
[34] M. S. Awan, "Cloud attenuations for free-space optical links," in *Proc. Int. Workshop Satell. Space Commun.*, Sep. 2009, pp. 274–278.
[35] M. A. A. Ali and A. Ali, "Performance analysis of fog effect on free space optical communication system," *IOSR J. Appl. Phys.*, vol. 7, no. 2, pp. 16–24, 2015.
[36] J. Li, J. Huang, K. Stamnes, T. Wang, Q. Lv, and H. Jin, "A global survey of cloud overlap based on CALIPSO and CloudSat measurements," *Atmos. Chem. Phys.*, vol. 15, no. 1, pp. 519–536, Jan. 2015.

JAVIER GARCÍA OLMEDO was born in Torrejón de Ardoz, Madrid, Spain, in 1996. He received the B.S. degree in telecommunication technologies engineering and the M.S. degree in science and technology from space from the University of Alcalá, in 2020 and 2022, respectively. He is currently pursuing the Ph.D. degree with the Multimedia and Communications Program, Universidad Carlos III de Madrid. His research interests include optical communication in inter-satellite and satellite-to-ground links.

VÍCTOR P. GIL JIMÉNEZ (Senior Member, IEEE) received the B.S. degree (Hons.) in telecommunication from the University of Alcalá, in 1998, and the M.S. degree (Hons.) in telecommunication and the Ph.D. degree (Hons.) from Universidad Carlos III de Madrid, in 2001 and 2005, respectively. He was with the Spanish Antarctica Base, in 1999, as a Communications Staff. He visited the University of Leeds, U.K., in 2003, Chalmers Technical University, Sweden, in 2004, and Instituto de Telecommunicaçoes, Portugal, from 2008 to 2010. He is currently with the Department of Signal Theory and Communications, Universidad Carlos III de Madrid, as an Associate Professor. He has also led several private and national Spanish projects and has participated in several European and international projects. He holds one patent. He has published over 80 journal articles/conference papers and nine book chapters. His research interests include advanced multicarrier systems for wireless radio, satellite, and visible light communications. He held the IEEE Spanish Communications and Signal Processing Joint Chapter Chair, from 2015 to 2023. He received the master's thesis and the Ph.D. thesis award from the Professional Association of Telecommunication Engineers of Spain, in 1998 and 2006, respectively.